

Multiphonon Scattering of Low-Energy Electrons*

ROBERT F. BARNES,† MAX G. LAGALLY, AND MAURICE B. WEBB

University of Wisconsin, Madison, Wisconsin 53706

(Received 30 January 1968)

The multiphonon scattering in low-energy electron diffraction experiments has been observed and analyzed. It is shown that the elastically scattered intensity integrated over a Brillouin zone is given by

$$\int_{\text{zone}} I_{\text{total}}(\mathbf{S}) d^2S \propto e^{-2M} \left(1 + 2M + \frac{(2M)^2}{2!} + \dots \right),$$

where $2M$ is the exponent in the Debye-Waller factor. The first two terms are the zero- and one-phonon terms, respectively; the remaining terms are the multiphonon scattering. The scattering from the (111) face of Ni has been measured. The observed diffuse intensity may be separated into two components: a uniform background which is a function of energy and temperature, and a remaining intensity which has all the properties expected of the one-phonon scattering. The uniform background is then shown to be the multiphonon scattering by comparing the results with the above relation using measured values of $2M$. The total elastic current integrated over back angles has been measured as a function of temperature and is essentially constant, as expected from above. It is thus possible to account for the phonon contribution in experiments to investigate other sources of diffuse scattering such as surface imperfections and amorphous layers of adsorbed foreign atoms.

I. INTRODUCTION

EARLIER, McKinney, Jones, and Webb¹ (hereafter referred to as II) reported the observation and analysis of the one-phonon thermal diffuse scattering from the (111) surface of Ag and showed that this first-order process gives a large contribution to the total scattering. Therefore one would expect appreciable intensity from higher-order or multiphonon scattering processes. Besides adding to the understanding of the scattering of slow electrons, knowledge of these processes will make it possible to correct for the phonon scattering in future experiments to investigate other sources of diffuse scattering such as surface disorder and imperfections and adsorbed layers of foreign atoms. It is the main purpose of this paper to report the observation of this multiphonon scattering.

In II the authors considered the diffuse scattering of nonpenetrating radiation from a surface layer of atoms which vibrate as bulk atoms of a solid described by a Debye spectrum in the high-temperature limit, but with a Debye temperature appropriate to the larger vibrational amplitudes of the surface. Using a pseudokinematic description of the scattering, they showed that the one-phonon thermal diffuse scattering for unit incident intensity should be given by

$$I_2(\mathbf{S}) = |f_0|^2 (e^{-2M}) \frac{N^2 k T d}{\pi m c^2} |\mathbf{S}|^2 \frac{1}{|\mathbf{S}_{11} - \mathbf{G}_{11}|} \times \tan^{-1} \frac{\pi}{d |\mathbf{S}_{11} - \mathbf{G}_{11}|}, \quad (1)$$

where f_0 is the atomic structure factor, e^{-2M} is the

* This work supported by the U. S. Air Force Office of Scientific Research under Grant No. AF-AFOSR-51-66.

† Present address: Plastics Department, DuPont Experimental Station, Wilmington, Del.

¹J. T. McKinney, E. R. Jones, and M. B. Webb, Phys. Rev. **160**, 523 (1967).

Debye-Waller factor, N is the number of atoms along the edge of the crystal, d is the lattice spacing, m is the mass of the atom, c is the sound velocity assumed to be the same for all polarizations and directions of propagation, k is the Boltzmann constant, T is the absolute temperature, $\mathbf{S} = \mathbf{k} - \mathbf{k}_0$ is the diffraction vector, where the \mathbf{k} 's are the propagation vectors of the scattered and incident beams, \mathbf{G} is a reciprocal-lattice vector, and the subscript \parallel indicates the components parallel to the surface.

As shown in II, the ratio of the one-phonon thermal diffuse scattering to the Bragg peak $I_1(\mathbf{S})$ is proportional to the temperature and to the square of the magnitude of the diffraction vector and, through much of the central region of the Brillouin zone, to the reciprocal of the distance from the tip of the diffraction vector to the nearest reciprocal-lattice rod.

In addition, it is shown in II that

$$R = \int_{\text{zone}} I_2(\mathbf{S}) d^2S / \int_{\text{zone}} I_1(\mathbf{S}) d^2S = 2M, \quad (2)$$

where R is the ratio of the integrated intensity in the one-phonon diffuse scattering to the integrated intensity in the associated Bragg peak, and $2M$ is the exponent in the Debye-Waller factor.²

Calculations of the one-phonon diffuse scattering explicitly including the force-free boundary conditions

² There is a correction to this statement. Actually $R = 2M(1 + \Delta)$. A part of Δ depends on the geometry of the particular experiment and arises from differences in elements of solid angle subtended at the crystal and at the origin of reciprocal space. Another part of Δ arises from the fact that as \mathbf{S} moves throughout the zone, phonons of different polarizations are sampled differently than in Debye-Waller measurements where $S_{11} = G_{11}$. Both these parts of Δ are of the order of q_{11}^2/G^2 averaged over the Brillouin zone. Even for the (333) reflection this factor is only about 1% and is less important for higher-order reflections. Neglecting this correction makes a negligible difference in any part of the analyses in the remainder of this paper.

have been made for an elastic continuum by Huber³ and for a model discrete lattice by Wallis and Maradudin.⁴ Their major results agree with those above in the central region of the zone about the (00) reciprocal-lattice rod.

In II the observed diffuse intensity from the (111) face of Ag is compared with Eqs. (1) and (2). In the Ag experiments there appeared to be a temperature-independent uniform background. After subtracting this background, the remaining intensity had the expected angular dependence in the central region of the Brillouin zone and had the correct temperature and energy dependence. The ratio of the integrated intensities in the diffuse scattering and in the Bragg peak was equal to the measured value of $2M$ within the experimental uncertainty.

McKinney *et al.* also considered the effect of the nonzero penetration of the elastically scattered electrons and showed that the penetration can change the angular dependence of the scattering in the outer regions of the Brillouin zone. This obscures any information about the phonon dispersion in the discrete lattice until the electron penetration is better understood.

In this paper we present the observations of the diffuse scattering from the (111) face of Ni. In Sec. II we present the experimental results, which unlike those for Ag show a background intensity that depends strongly on both the energy and the temperature; in Sec. III we show that it is possible to subtract a uniform background, leaving a remaining intensity which has all the properties expected for the one-phonon diffuse scattering; and in Sec. IV we arrive at an expression for the integrated intensity for all orders of the multiphonon scattering, and show that the background which has been subtracted is this multiphonon scattering. Then we comment on the background in the Ag experiments.

II. EXPERIMENTAL

The apparatus used in many of these experiments was described previously.^{1,5} Briefly, the crystal is mounted on a two-circle goniometer with a tilt axis lying in the plane of the crystal surface and an azimuthal axis normal to the surface. The crystal can be heated from underneath by radiation and electron bombardment. The scattered electrons are detected in a Faraday cage which rotates about the tilt axis of the goniometer. The detector aperture is a slit with its long axis parallel with the tilt axis, and subtends 5×40 mrad at the crystal. Observed diffraction maxima obtained by changing the crystal tilt have a full width at half-maximum of 13 mrad, which is almost entirely due to the instrumental width. The collector is biased 1.5 V positive with respect to the electron gun filament to accept only elastically⁶ scattered electrons. There is also a fluorescent

screen behind closely spaced grids for visual observation of the diffraction. The system is pumped with a glass orbitron pump, and indicated pressures after bakeout were 2×10^{-10} Torr or lower.

In Sec. IV we discuss measurements of the integrated elastically scattered current. These experiments were done in a new apparatus similar to the one above but which also has the usual⁷ closely spaced hemispherical grids in front of a fluorescent screen. A thin phosphor coat is deposited on a conducting glass envelope which serves as the collector in these experiments. With the retarding grid biased to pass only the elastically scattered electrons and the fluorescent screen at the crystal potential to collect any secondary electrons ejected from it, the current to the screen is the elastically scattered intensity integrated over back angles. The collector actually subtends 140° and has a small hole to admit the incident beam.

The crystals used in these experiments were 99.997% Ni obtained from Materials Research Corporation. Surfaces parallel to the (111) planes to within $\frac{1}{2}^\circ$ were prepared by mechanical polishing and etching in a solution of 13 parts acetic acid, 7 parts nitric acid, and 0.1 part hydrochloric acid. After mounting the crystal and achieving good vacuum, the temperature of the crystal was pulsed above 650°C until only those diffraction spots expected from the clean (111) Ni surface were observed. After some time without heating, weak fractional-order spots were observed and could be removed by repeating the temperature pulses. Occasionally, and usually after opening the system to air, this procedure did not produce a clean crystal and then the procedures described by MacRae⁸ and by Germer and MacRae⁹ were employed. The experiments to be reported here were done on surfaces for which no fractional-order diffraction maxima were observed. Fractional-order peaks with intensities 0.05% of the clean-Ni diffraction peaks would have been detected.

Measurements of the Debye-Waller factor were made at positions of the third-Laue-condition maxima along the (00) reciprocal-lattice rod.¹⁰ These experiments are essentially the same as those described for Ag by Jones, McKinney, and Webb.⁵ Except that we shall use some of the resulting values of $2M$, these experiments and their analysis will not be discussed here.

The geometry of the experiments to measure the diffuse scattering is shown in Fig. 1. The diffraction vector \mathbf{S} is swept across the (00) reciprocal-lattice rod at the positions of the third-Laue-condition maxima.

energy has changed by the order of phonon energies. This corresponds to the experimental situation in low-energy electron diffraction experiments, where the energy resolution is limited by the thermal spread from the electron source.

⁷ E. J. Scheibner, L. H. Germer, and C. D. Hartman, *Rev. Sci. Instr.* **31**, 112 (1960); **31**, 675 (1960).

⁸ A. U. MacRae, *Surface Sci.* **1**, 319 (1964).

⁹ L. H. Germer and A. U. MacRae, *J. Appl. Phys.* **33**, 2923 (1962).

¹⁰ R. F. Barnes, Ph.D. thesis, University of Wisconsin (unpublished).

³ D. L. Huber, *Phys. Rev.* **153**, 772 (1967).

⁴ R. F. Wallis and A. A. Maradudin, *Phys. Rev.* **148**, 962 (1966).

⁵ E. R. Jones, J. T. McKinney, and M. B. Webb, *Phys. Rev.* **151**, 476 (1966).

⁶ We include in the "elastically scattered electrons" those whose

The angle ψ is taken as a measure of $|\mathbf{S}_{11}-\mathbf{G}_{11}|$. As discussed in II, this procedure holds the scattering angle 2θ fixed and eliminates the angular dependence of the atomic structure factor $f(\theta, E)$. The resulting diffuse scattering is very nearly symmetric about the (00) reciprocal-lattice rod.

Log-log plots of the measured intensity for several temperatures and incident-electron energies are shown in Figs. 2 and 3. The figures show that the magnitude of the slope of the diffuse intensity decreases with both increasing temperature and incident energy.

III. ONE-PHONON SCATTERING

Clearly the data for Ni are more complicated than for Ag in that it is not possible to subtract a temperature-independent uniform background and obtain the one-phonon scattering. Therefore, we ask: Is there a uniform background at each temperature and energy which when subtracted leaves the remaining intensity with a ψ^{-1} angular dependence in the central region of the Brillouin zone; and, if so, does this remaining intensity have the other properties expected for the one-phonon scattering? An example of such a separation of the data is shown in Fig. 4 for the (666) reflection at 443°K. Subtraction of $I_B=1.4\times 10^{-13}$ A leaves a remaining intensity which goes as ψ^{-1} three quarters of the way to the zone boundary. It would perhaps be better to make a somewhat larger subtraction, both because Eq. (1) gives $I_2 \propto \psi^{-1} \tan^{-1}(\psi_{ZB}/\psi)$, where ψ_{ZB} is the value of ψ at the zone boundary, and because I_2 should decrease faster than ψ^{-1} for slightly penetrating radiation. On the other hand, phonon dispersion will make I_2 less steep than ψ^{-1} near the zone boundary. For the data in Fig. 4, subtraction of 1.6×10^{-13} A leaves a reasonable fit either to $\psi^{-1} \tan^{-1}(\psi_{ZB}/\psi)$ or to the angular dependence of I_2 estimated in II for slightly penetrating radiation. Since these effects are not well known we proceed using the subtraction which gives ψ^{-1} in the central region of the zone and take the differences between the above subtractions as a rough measure of the uncertainties due to this procedure.

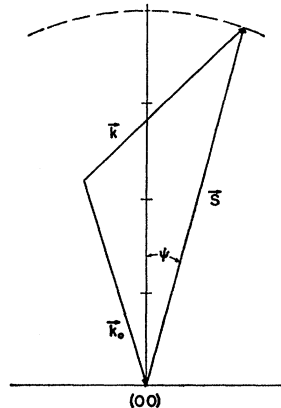


FIG. 1. Geometry of the experiments to measure the diffuse intensity near the (00) reciprocal-lattice rod. The triangle \mathbf{k} , \mathbf{k}_0 , and \mathbf{S} is rigid and ψ is changed by tilting the crystal. The dotted line is the path of the detector.

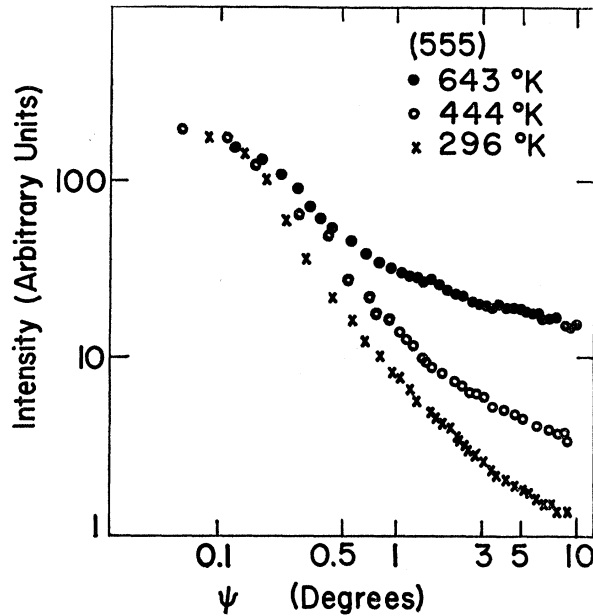


FIG. 2. Scattered intensity versus ψ at several temperatures. The detector crosses the (00) reciprocal-lattice rod at the position of the (555) reflection. The scattering angle is 158° and the energy is 208 eV. The curves are normalized at $\psi=0$.

We now compare the intensity remaining after the background subtraction to that expected for the one-phonon scattering. This comparison is made at ψ

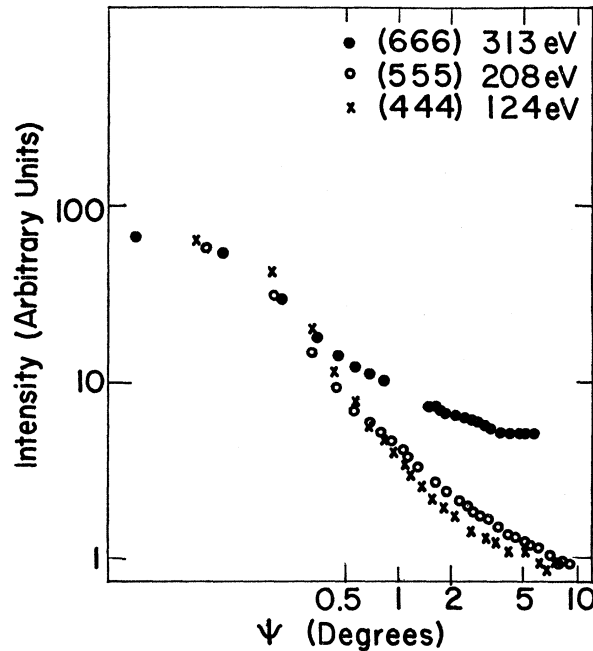


FIG. 3. Scattered intensity versus ψ at several incident energies. The detector crosses the (00) reciprocal-lattice rod at the position of the (444), (555), and (666) reflections. The scattering angle is 158° and the temperature is 643°K. The curves are normalized at $\psi=0$.

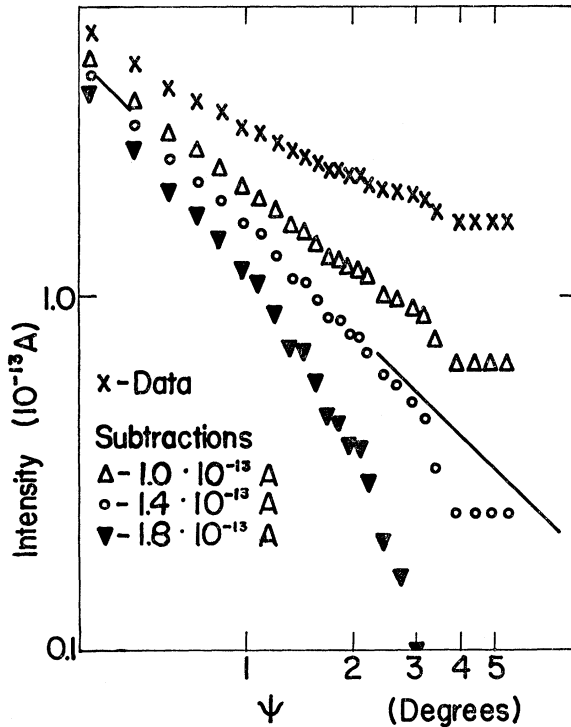


FIG. 4. Scattered intensity versus ψ with background subtractions. The measured intensity is indicated by the \times 's. Other symbols indicate the intensity remaining after subtracting various uniform backgrounds. The data are for the detector crossing the (00) reciprocal-lattice rod at the position of the (666) reflection. The scattering angle is 158° , $E=313$ eV, and $T=443^\circ\text{K}$.

$=0.2\psi_{ZB}$, where both the background uncertainty and wings of the Bragg peak are small. In Fig. 5 the ratio of the remaining diffuse intensity at $0.2\psi_{ZB}$ to the maximum intensity in the associated Bragg peak is plotted against the temperature. The straight lines through the origin are drawn as visual fits to the data. For the lowest-order reflection the diffuse scattering is small and con-

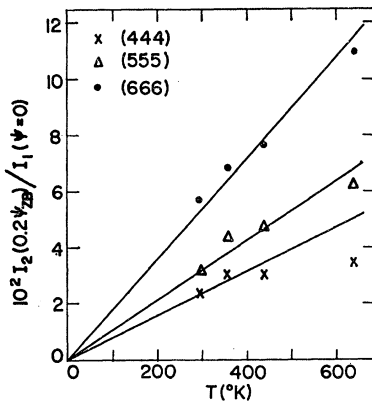


FIG. 5. Temperature dependence of the ψ^{-1} component. $I_2(\psi=0.2\psi_{ZB})/I_1(\psi=0)$ is plotted as a function of temperature for various reflections on the (00) reciprocal-lattice rod. The lines are visual fits through the origin.

sequently the scatter is large. Within the experimental uncertainties the ratio is proportional to the temperature in agreement with Eq. (1).

Equation (1) also predicts this ratio to be proportional to $|\mathbf{S}|^2$. We check this by plotting the slopes of the lines in Fig. 5 against the magnitude of the diffraction vector \mathbf{S} . The results on a log-log plot are shown in Fig. 6, where the solid line is drawn with the expected slope 2.

To check the magnitude of the ψ^{-1} component, we wish to compare the results with Eq. (2). The ratio of the integrated intensities in the diffuse and Bragg scattering is difficult to determine experimentally¹ because neither the shape of the Bragg peak nor of the instrumental function is well known, and slit corrections, important for the sharp peak, cannot be made accurately. Using the procedures of II we estimate that $0.84(2M) < R < 1.86(2M)$. In a later section we return to the question of the integrated intensities.

Thus we conclude that the ψ^{-1} component of the diffuse scattering does have the other properties of the one-phonon thermal diffuse scattering.

IV. MULTIPHONON SCATTERING

We now consider the background intensity and identify it as the multiphonon scattering.

There is a particularly simple way to arrive at the expected integrated intensity in the multiphonon scattering and some of its other properties. The one-phonon scattering is a distribution of sidebands in the perfect-lattice scattering, each sideband arising from the periodic modulation of the lattice by phonons of a particular wave-vector component \mathbf{q}_{11} . Just like the Bragg peak, these one-phonon sidebands will have their own sidebands due to other phonons. These second sidebands are the two-phonon contributions to the diffuse scattering, and so forth, for higher orders.

$$R = \int_{\text{zone}} I_2(\mathbf{S}) d^3S / \int_{\text{zone}} I_1(\mathbf{S}) d^3S = 2M \quad (2)$$

relates the integrated intensity in a peak to the integrated intensity in its one-phonon sidebands and is true even if the peak is itself a sideband of another. Therefore the integrated intensity in the two-phonon scattering is $\frac{1}{2}(2M)^2$ times the integrated intensity in the Bragg peak. The factor of $\frac{1}{2}$ is included to avoid

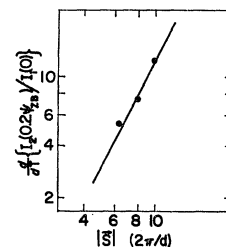


FIG. 6. Dependence of the ψ^{-1} component on the magnitude of \mathbf{S} . The slopes of the lines in Fig. 5 are plotted versus $|\mathbf{S}|$. The straight line has slope 2.

counting the contribution from each pair of phonons twice. The n -phonon-scattering integrated intensity is then $(2M)^n/n!$ times the Bragg peak and the entire integrated intensity is

$$\int_{\text{zone}} I_{\text{total}}(\mathbf{S}) d^2S \propto e^{-2M} \times \left(1 + 2M + \frac{(2M)^2}{2!} + \cdots + \frac{(2M)^n}{n!} + \cdots \right). \quad (3)$$

Terms 1 and $2M$ are the integrated zero- and one-phonon contributions.¹¹ Therefore,

$$\int_{\text{zone}} I_M(\mathbf{S}) d^2S \propto e^{-2M} (e^{2M} - 1 - 2M) \quad (4)$$

is the integrated intensity of the multiphonon scattering. The total integrated scattering is independent of $2M$ and thus of the position of the atoms.

This expression says nothing about the distribution of $I_M(\mathbf{S})$ throughout the Brillouin zone. However, in the last section it was established that subtracting a uniform background leaves a remaining intensity with the properties of $I_2(\mathbf{S})$. If we wish to associate this background with $I_M(\mathbf{S})$, the multiphonon scattering would have to be uniform in the zone to within the uncertainty in the shape of $I_2(\mathbf{S})$. We proceed as if this were so, and the consistency of the results will support this assumption.

This assumption is also supported by a detailed calculation of the two-phonon scattering, only the results of which will be presented here. The details are given in Ref. 10. Using Eq. (5.26) of James,¹² expanding the second exponential factor, and collecting all terms involving two phonons gives, for the two-phonon scattering $I_3(\mathbf{S})$,

$$I_3(\mathbf{S}) \propto (e^{-2M}) \frac{1}{128} \sum_{qz} \sum_{q'z'} (\mathbf{S} \cdot \mathbf{e}_{qz})^2 (\mathbf{S} \cdot \mathbf{e}_{q'z'})^2 \langle u_{qz}^2 \rangle \langle u_{q'z'}^2 \rangle^2 \times [I_0(\mathbf{S} + \mathbf{q} + \mathbf{q}') + I_0(\mathbf{S} + \mathbf{q} - \mathbf{q}') + I_0(\mathbf{S} - \mathbf{q} + \mathbf{q}') + I_0(\mathbf{S} - \mathbf{q} - \mathbf{q}')], \quad (5)$$

where \mathbf{q} is the phonon wave vector, z is a polarization index, \mathbf{e}_{qz} is the unit polarization vector, and $\langle u_{qz}^2 \rangle$ is the thermal average of the square of the amplitude of the qz th mode. Then assuming $\langle u_{qz}^2 \rangle = \langle u_{-qz}^2 \rangle$ and considering scattering from a single plane of atoms which vibrate as bulk atoms with a Debye spectrum in the high-temperature limit, one obtains

$$I_3(\mathbf{S}) \propto \frac{1}{2} (e^{-2M}) T^2 |\mathbf{S}|^4 \sum_{\mathbf{q}} \sum_{\mathbf{q}'} \frac{I_0(\mathbf{S}_{11} - \mathbf{q}_{11} - \mathbf{q}'_1)}{(q_{11}^2 + q_1^2)(q'_{11}{}^2 + q'_1{}^2)}, \quad (6)$$

¹¹ The same expression for x rays is given by S. V. Semenovskaya and Ya. S. Umanskiĭ, *Fiz. Tverd. Tela* **6**, 2963 (1964) [English transl.: *Soviet Phys.—Solid State* **6**, 2362 (1965)].

¹² R. W. James, *The Optical Principles of the Diffraction of X Rays* (G. Bell and Sons, London, 1962).

where we have averaged over phonon polarizations and velocities. Replacing the sums by integrations over Brillouin zones and using the fact that $I_0(\mathbf{S}_{11})$ is a periodic δ function, the expression to be evaluated is

$$I_3(\mathbf{S}) \propto \frac{1}{2} (e^{-2M}) T^2 |\mathbf{S}|^4 \sum_{\mathbf{G}_{11}} \int_{\text{zone}} d^2q_{11} \int_{-\pi/d}^{\pi/d} \frac{dq_1}{(q_{11}^2 + q_1^2)} \times \int_{-\pi/d}^{\pi/d} \frac{dq'_1}{(\mathbf{S}_{11} - \mathbf{q}_{11} - \mathbf{G}_{11})^2 + q'_1{}^2}. \quad (7)$$

The integrations have been estimated using a combination of analytical and numerical methods, approximating for the limits of integration, and considering only normal processes in the zone about the (00) reciprocal-lattice rod. The result is a complicated expression but can be approximated by $I_3(\mathbf{S}) \approx e^{-(0.24/\psi ZB)}$. Consideration of umklapp processes and the effects of the approximate limits of integration suggests that $I_3(\mathbf{S})$ should be even more uniform than this result. Presumably higher-order terms also give nearly uniform scattering. No calculation of the shape of the multiphonon scattering of slightly penetrating radiation has been made.

We now wish to compare the experimental background I_B with Eq. (4). If I_B is the multiphonon scattering, then

$$\int_{\text{zone}} I_B d^2S / \int_{\text{zone}} I_1(\mathbf{S}) d^2S = (e^{2M} - 1 - 2M), \quad (8)$$

where forming the ratio has eliminated the need to know the incident intensity and quantities depending on the crystal. All terms appearing in Eq. (8) are experimentally available and there are no adjustable parameters. However, an uncertainty arises in determining the experimental value of $\int I_1(\mathbf{S}) d^2S$ because of slit corrections. This uncertainty leads to ratios of integrated intensities in error by the same factor at all temperatures and energies since the observed shape of $I_1(\mathbf{S})$ does not change with these variables. Therefore the temperature and energy dependences of intensity ratios are more reliable than their absolute values. Consequently, we temporarily introduce a proportionality factor β in the right-hand side of Eq. (8) and discuss the absolute intensity in a later paragraph.

The integration of $I_M(\mathbf{S})$ over the zone is straightforward. The integration over the Bragg peak is discussed in II. The values of $2M$ are available from the Debye-Waller measurements. In Fig. 7 the ratio of the integrated intensities is plotted as a function of temperature for the (666) reflection at an energy of 313 eV and a grazing angle of incidence of 79°. The solid line in Fig. 7 is a plot of $\beta(e^{2M} - 1 - 2M)$ with the value of $2M = 7.25 \times 10^{-3} T$ taken from the Debye-Waller measurements, and with $\beta = 0.53$ chosen so the curve agrees with the point at 443°K.

In Fig. 8 the dots are the ratios of the integrated

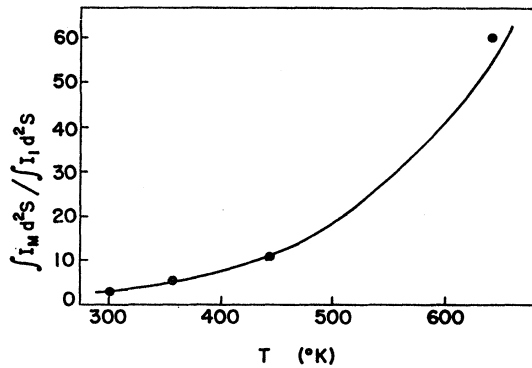


FIG. 7. Temperature dependence of the multiphonon scattering. The points are experimental values of $\int I_M(\mathbf{S})d^2S/\int I_1(\mathbf{S})d^2S$ for the (666) reflection at various temperatures. $2\theta=158^\circ$, $E=313$ eV. The solid line is a plot of $\beta(e^{2M}-1-2M)$ for $2M=7.25 \times 10^{-3} T$, and $\beta=0.53$ chosen so the function agrees with the data point at 443°K. Errors in the data points are $\approx \pm 15\%$ at $T=300^\circ\text{K}$ and $\approx \pm 5\%$ at $T=643^\circ\text{K}$. Errors in measured values of $2M$ are $\approx \pm 12\%$.

intensities at 643°K plotted versus the electron energy for several reflections on the (00) reciprocal-lattice rod. The dashed line connects values of 0.53 ($e^{2M}-1-2M$), using the $2M$'s measured for these same reflections. The proportionality constant is the same as used for Fig. 7. Similar comparisons for data at lower energies and temperatures give similar agreement but with somewhat larger scatter since the background intensities are smaller.

We now consider the absolute ratios of the integrated intensities. These ratios are smaller than expected by the factor $\beta=0.53$, which is within the uncertainties of determining $\int I_1(\mathbf{S})d^2S$, and thus the results are consistent with the expectations.

However, there is a different way to check the relative magnitudes of the various components of the scattering; that is to measure directly the integrated elastically scattered intensity as a function of temperature, which Eq. (3) predicts to be constant.

We require a measurement over the Brillouin zone but we collect current over all back angles. The corresponding region in reciprocal space is not bounded by zone boundaries. This will lead to small variations

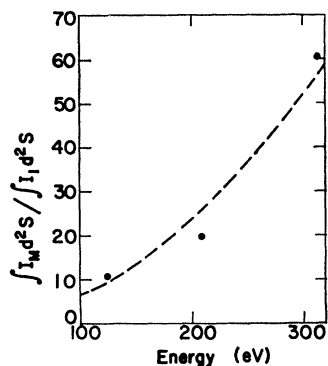


FIG. 8. Energy dependence of the multiphonon scattering. The points are experimental values of $\int I_M(\mathbf{S})d^2S/\int I_1(\mathbf{S})d^2S$ for the (444), (555), and (666) reflections at $T=643^\circ\text{K}$, $2\theta=158^\circ$. The dashed line connects values of $\beta(e^{2M}-1-2M)$ using $2M$ measured for each reflection. $\beta=0.53$, $2\theta=158^\circ$, $T=643^\circ\text{K}$.

in the integrated current with temperature. Consider an energy where several reciprocal-lattice rods lie just inside the Ewald sphere. As the temperature is increased, intensity is removed from these Bragg peaks and is spread throughout their associated zones so that some of this intensity will no longer be collected. Alternatively, at a somewhat lower energy, these several rods will lie outside the sphere, and with increasing temperature some of the associated diffuse scattering will be added to the measured current. The size of this effect is difficult to calculate accurately, but for our present purpose the following estimate is sufficient: We neglect variations in the atomic structure factor and assume zero electron penetration,¹³ and then ask for the expected change in the integrated current going from zero to infinite temperature. This will overestimate the size of the effect. If there are n rods in the circle of radius $|\mathbf{k}_0|$, the integrated current at $T=0^\circ\text{K}$ will be n times the Bragg peak in the diffraction from the rigid lattice. At $T=\infty$ the intensity of a Bragg peak will be spread uniformly through the area of the associated zone, $\frac{1}{2}\sqrt{3}|\mathbf{a}^*|^2$, where \mathbf{a}^* is the reciprocal-lattice basis vector. The collected current will then be $\pi|\mathbf{k}_0|^2$ times this current density in reciprocal space. Therefore the ratio of the currents at $T=0^\circ\text{K}$ and $T=\infty$ will be $\sqrt{3}n|\mathbf{a}^*|^2/2\pi|\mathbf{k}_0|^2$. For example, at normal incidence and 100 eV, this ratio is 1.17, and at 350 eV it is 0.94, so the edge effects are small.

In Fig. 9 recorder traces of the integrated intensity versus temperature are reproduced for three incident energies. The middle trace is at 194 eV, an energy chosen so that the above ratio is unity.¹⁴ The curves for higher and lower energy show the edge effects. For the above energy and temperature range, the Debye-Waller factor reduces the Bragg intensity to $\approx 3\%$ of its room-temperature value. Indeed the integrated current is essentially constant with temperature as predicted by Eq. (3).

Previously we separated the observed intensity into three components and showed that these individually have the temperature dependences expected for the zero-, one-, and multiphonon contributions. Now it is shown that their sum, the integrated current, has the expected temperature dependence. This can be true only if the relative magnitudes of the three components are correct. We estimate that discrepancies in the coefficients of the three components larger than 20% would not be consistent with the data and uncertainties. Thus the factor $\beta=0.53$ must indeed be due to the difficulties in integrating $I_1(\mathbf{S})$.

¹³ The modulation of the interference function along the reciprocal-lattice rods due to the electron penetration can give another edge effect in the integrated current as a function of temperature. This arises because the phonon scattering is more uniform in the direction of the rods than is the no-phonon scattering.

¹⁴ Actually the energy was chosen from a similar expression which accounts for the fact that the screen subtends 140° instead of 180° .

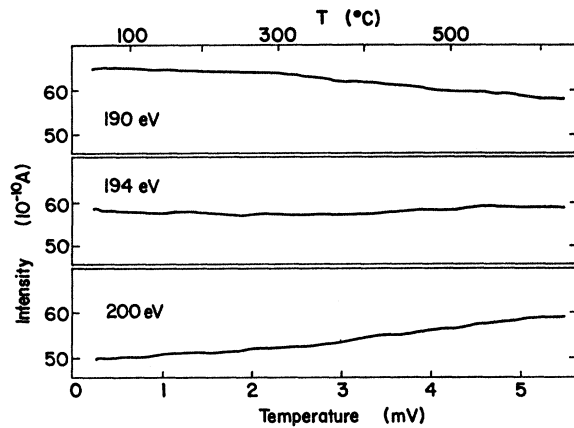


FIG. 9. Integrated elastically scattered current as a function of temperature. Reproduction of recorder traces of the elastically scattered current collected over all back angles versus the thermocouple emf at several energies.

We now reexamine the data for the (111) surface of Ag, which must also show the multiphonon scattering. In II a temperature-independent background was subtracted from the diffuse intensity. This was supported by the observation, demonstrated in Fig. 6 of that paper, that the intensity near the zone boundary was temperature-independent within the uncertainty. However, using the same procedure as in this paper, we ask for a background subtraction which leaves a remaining ψ^{-1} component in the region $0 < \psi < (\frac{3}{4})\psi_{ZB}$. For the data in Fig. 6 of II this gives $I_B = 1.6 \times 10^{-13}$ A at 282°C and $I_B = 1.1 \times 10^{-13}$ A at $T = 22^\circ\text{C}$ and the resulting ratios $I_B/I_1(\psi=0)$ are indeed proportional to $(e^{2M} - 1 - 2M)$. A more sensitive check can be made for the (666) reflection where $2M$ is considerably larger. This comparison is shown in Fig. 10. The data have been normalized at 389°K . Thus the expected multiphonon scattering is present in the Ag data although it is more difficult to

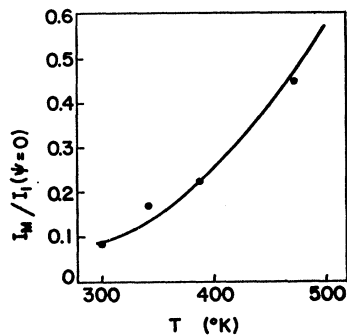


FIG. 10. Temperature dependence of the multiphonon scattering from (111) Ag. The ratio $I_M/I_1(\psi=0)$ is plotted versus temperature for the (666) reflection from Ag, $2\theta = 170^\circ$, $E = 240.5$ eV. The line is a plot of $\beta(e^{2M} - 1 - 2M)$ using the measured value of $2M = 8.17 \times 10^{-3}T$. β has been chosen so the function agrees with the data point at 389°K .

observe because of the generally smaller values of $2M$. This leaves the question of the temperature independence of the measured intensity at the zone boundary. There the intensity consists of both one- and multiphonon scattering, which have opposite variations with temperature. The relative amounts of these two intensities are not known at the zone boundary, but an upper limit to the expected temperature dependence is obtained by assuming the entire intensity is multiphonon. In this case the current at 282°C should be 0.3×10^{-13} A greater than at 22°C , which is just outside the experimental uncertainty in the data.

V. DISCUSSION

In all respects then, the observed diffuse intensity agrees with the expectations from the simple analysis and there can be no doubt that it represents the one- and multiphonon scattering. Perhaps the most surprising result of the present work is that the simple ideas work so well. The analysis has been based on a pseudo-kinematic description of the diffraction, it has neglected the nonzero penetration of the electrons, it assumed a simplified model of the surface lattice dynamics and uniform multiphonon scattering. Further, there is a question of what value of $2M$ should be used in the comparison in Eq. (8). As was pointed out in II, the phonon scattering "sees" the outermost layer of atoms with its larger $2M$ more strongly than does the Bragg scattering. In view of these approximations it should be emphasized that the present work points out only some of the major features of the multiphonon scattering. These effects are being investigated further.

It is interesting to point out that the phonon scattering is a very large contribution to the total scattering. For example, even at 100 eV and room temperature, the Bragg peak contains only about $\frac{1}{3}$ of the elastic current. This fact should be accounted for in making dynamical theories of the diffraction or at least in comparing them with room-temperature data.¹⁵

It is clear that $I_M(S)$ cannot be strictly uniform in the zone since even at high temperatures, where the scattering is essentially all in the multiphonon component, it must at least reflect the pair distribution function of the atoms and the short range order. Experiments with this point of view are in progress.

The observations of the multiphonon scattering do not provide a very useful tool to study details of the surface lattice dynamics, but they must be understood before the diffuse scattering may be used to investigate other phenomena such as surface disorder and imperfections, amorphous layers of adsorbed atoms, and the one-phonon diffuse scattering itself.

¹⁵ F. Hofmann and H. P. Smith, Jr., Phys. Rev. Letters 19, 1472 (1967). Property 4 of the model in this reference would be appropriate only at low temperatures.